

# Kinematic Precise Point Positioning (PPP) Solution for Hydrographic Applications

Ashraf ABDALLAH and Volker SCHWIEGER, Germany

**Keywords:** Kinematic GNSS-PPP, Hydrographic Applications, Bernese Software

## SUMMARY

Precise Point Positioning (PPP) has been one of the major research areas in surveying in recent years to obtain cost effectively coordinates using one dual frequency GNSS instrument. The purpose of this study is to investigate the accuracy of the kinematic PPP solution using Bernese software for hydrographic applications. This PPP solution was compared with the double-difference solution from Bernese software. The Virtual **SAPOS** (SAtellitenPOSitionierungsdienst der deutschen Landesvermessung) reference station was considered as a reference station.

Two kinematic trajectories have been observed within project “HydrOs (Integrated Hydrographic Positioning System) on the Rhine River, Duisburg, Germany. This project is launched in co-operation of the department M5 (Geodesy) of the German Federal Institute of Hydrology (BfG) and the Institute of Engineering Geodesy at the University of Stuttgart (IIGS).

The first kinematic trajectory shows a standard deviation for the kinematic PPP solution of 6 cm in East, 2.1 cm in North, and 6.8 cm in height. If the 5% of the measurements are eliminated as outliers, the standard deviation values for a confidence level of 95% ( $SD_{95\%}$ ) are 5 cm in East, 1.2 cm in North and 5 cm in height. The second trajectory, which started with 40 minutes of quasi-static observation time (non-moving vessel), achieves a more precise solution. The standard deviation values of all measurement are 1.7 cm in East, 2.6 cm in North, and 4.9 cm in height. For a confidence level of 95%, the PPP solution provides a standard deviation ( $SD_{95\%}$ ) of 1.5 cm for the East and North directions. Moreover, it delivers 3 cm for the height.

# Kinematic Precise Point Positioning (PPP) Solution for Hydrographic Applications

Ashraf ABDALLAH and Volker SCHWIEGER, Germany

## 1. INTRODUCTION

The GNSS Precise Point Positioning (PPP) technique is one of the most challenging surveying methodologies to achieve a high accurate positioning. In addition, it provides the advantage of using one dual GNSS instrument (GOA, 2006). The estimation of PPP solution is based on the ionosphere-free linear combination for code data ( $\rho_{IF}$ ) and carrier phase data ( $\Phi_{IF}$ ). These linear combinations are formed in equations (1) & (2). The ambiguity ( $N_{IF}$ ) for  $L_1$  ( $f_{L1}$ ) and  $L_2$  ( $f_{L2}$ ) signals is no longer an integer (float solution) and will be constant as long as no loss of lock in carrier phase occurs.  $r$  refers to the true geometric range between the satellite and receiver; the clock offset for receiver and satellite are defined by  $\delta^R$  and,  $\delta^S$  and  $c$  indicates the light speed.  $\lambda_{IF}$  symbolize the combined carrier wavelength. (MIRSA & ENGE, 2010)

$$\rho_{IF} = \frac{f_{L1}^2}{(f_{L1}^2 - f_{L2}^2)} \rho_{L1} - \frac{f_{L2}^2}{(f_{L1}^2 - f_{L2}^2)} \rho_{L2} = r + c(\delta^R - \delta^S) + T_z \cdot m(el) \quad (1)$$

$$\phi_{IF} = \frac{f_{L1}^2}{(f_{L1}^2 - f_{L2}^2)} \phi_{L1} - \frac{f_{L2}^2}{(f_{L1}^2 - f_{L2}^2)} \phi_{L2} = r + c(\delta^R - \delta^S) + T_z \cdot m(el) + \lambda_{IF} \cdot N_{IF} \quad (2)$$

The ionosphere-free combination eliminates the first order ionospheric error. Therefore a higher order ionospheric terms are used (KEDER, ET AL., 2003); the related equations are reported in BASSIRI & HAJJ (1993). The troposphere refraction is modeled in the equations (1) & (2) with term of ( $T_z \cdot m(el)$ ), which refers to the troposphere delay including the mapping function. The troposphere delay consists of two components. The hydrostatic dry delay, which could be predicted and includes nearly 90 % of the troposphere delay (HOFFMANN-WELLENHOF ET AL., 2000). The second part is called the wet component and it is not easy to predict (LEICK, 1995). For further information regarding troposphere delay modelling, it is recommended to see HOPFIELD (1969), MARINI (1972), NIELL (1992) and SAASTAMOINEN (1973). In addition to precise orbit and satellite clock data, other biases should be considered to obtain a highly PPP accuracy such as the absolute phase center variation for satellite and receiver antenna (PCV), atmosphere tidal loading and ocean tidal effects.

With respect to the hydrographic applications, several researchers have investigated the PPP technique. BÖDER (2010.a) has investigated the PPP solution for four antennas onboard a survey vessel. The PPP solution is compared to the Real Time Kinematic (RTK) solution for hydrographic applications on the Elbe River. The PPP solution was carried out by the software modules Wapp and TripleP, which are implemented in the Technical University of

Dresden, Germany. The error's mean value in the East direction is equal to 13.4 cm with a standard deviation (SD) of 3.5 cm. In the North direction, the mean error is calculated to 3.10 cm (SD = 6.60 cm) and in the height direction of 19.20 cm (SD = 9.40 cm). Furthermore, BÖDER (2010.b) has presented for the same experiment a different results with mean error in East of 0.5 cm (SD = 1.1 cm). In the North direction, the mean error is equal 1.90 cm (SD of 1.40 cm) and 6.90 cm (SD = 2.1 cm) for height. HESSELBARTH (2011) has reported a comparison between the kinematic PPP solution and DGNSS solution for 8 kinematic trajectories between July and September 2009 in the Baltic sea (open ocean). The DGNSS solution was obtained using WA1 software, which was developed by Lambert Wanninger, the Technical University of Dresden, Germany. The PPP solution is provided using the software modules Wapp and TripleP. The GPS kinematic PPP solution provided a mean standard deviation of 1.20 and 1.70 for East and North. Furthermore, it delivered 5.0 cm in height.

ALKAN & ÖCALAN (2013) have assessed the PPP solution in marine application. The test was carried out in August 2009 in Halic Bay, Istanbul, Turkey. Leica Geo-Office software was used to obtain the reference DGNSS solution and the observation data was processed using CSRS-PPP online service to get the PPP solution. The kinematic PPP solution was compared to DGNSS solution and it gave a position accuracy of 15 cm and up to 25 cm for height. MARREIROS, ET AL. (2012) has studied the PPP solution for marine applications; these kinematic PPP results are compared to RTK solution. The PPP solution has provided a decimetre accuracy level for ellipsoidal height comparison. Additionally, MOREIRA, ET AL. (2012) has examined the capability of PPP solution for remote platforms in Amazon basin. The research found that PPP solution is very useful for hydrographical application in Amazon River.

The major objective of this study is to investigate the accuracy of kinematic PPP solution for the hydrographic applications for the rivers. Throughout this paper, Bernese software V. 5.2 is used to process the measurement data for the PPP and double-difference solutions. One of the research issues of this paper is to prove the suitability of Bernese software for kinematic PPP for hydrographic application. The experimental approach taken in this study is observed as a part of project "HydrOs - Integrated Hydrographical Positioning System". Two trajectories have been observed on the Rhine River, Duisburg, Germany through this project.

## **2. GNSS SOLUTION USING BERNESE SOFTWARE**

### **2.1 Overview of Bernese software**

Bernese software V. 5.2 is high quality GNSS processing software using the post processing mode. It provides the possibility to process the GNSS measurement data for the static and kinematic surveying. Furthermore, it processes the data in double-difference (Differential GNSS) and zero-difference (PPP solution) techniques. This software is developed at the Astronomical Institute of the University of Bern (AIUB), Switzerland (DACH ET AL., 2007). The documentation of the software is available in a user manual, which is available online in PDF format. Moreover, a tutorial course is available which is related to data processing under DACH & WALSER (2014).

Table 1 compares the different frequency types in Bernese software.  $L_1$  and  $L_2$  refer to the default GNSS signals,  $L_3$  is the ionospheric free linear combination, and  $L_4$  is the geometry

free combination. The wide lane combination for dual measurement data is defined as  $L_5$  combination. In addition,  $L_6$  refers to the Melbourne-Wübbena combination (MELBOURNE, 1985; WÜBBENA, 1985; DACH ET AL., 2007). The main estimation in Bernese software is carried through the ionosphere-free dual combination ( $L_3$ ). The outlier and cycle slip detection, repairing of cycle slip and smoothing of code observations are estimated using  $L_4$ ,  $L_5$ , and  $L_6$  combinations.

Table 1 : Bernese frequencies (DACH ET AL., 2007)

Function Part	Definition
$L_1$	First frequency
$L_2$	Second frequency
$L_3$	Ionosphere-free combination for dual data, [narrow-lane]
$L_4$	Geometry- free combination
$L_5$	Wide-lane combination for dual data
$L_6$	Melbourne-Wübbena combination for dual data [wide-lane]

## 2.2 Processing using Bernese software for Double-Difference and Zero-Difference

Bernese software contains a group of different tools, which are called programs to complete the processing for double-difference or zero-difference mode. The estimation of the two techniques has the same processing schedule in most of the pre-processing stages. The change appears later within the parameter estimations section.

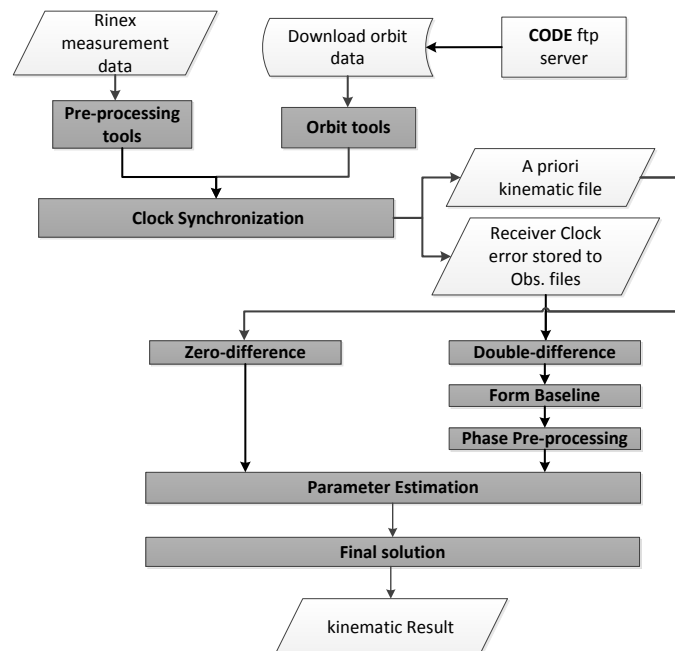


Figure 1 : Bernese software processing schedule

As shown in Figure 1, the processing starts with downloading the related orbits from the CODE (Center for Orbit Determination in Europe) ftp server (CODE, 2014). The orbit tools include the updating of the Earth orientation parameters to be in Bernese format (**POLUPD**

program), converting the satellite data to a specific format (**PRETAB** program) and generating the standard orbit format for Bernese software (**ORBGEN** program). Regarding the preprocessing tools, the **RNXSMT** program contains the smoothing of the Rinex data from outliers and cycle slips.

Furthermore, this smoothing step is followed by converting the Rinex into Bernese binary format (**RXOBV3** program). The receiver clock is synchronized with respect to the GPS time and stored to observation files using the Clock synchronization tools (**CODSPP** program). Using the code solution, a priori kinematic file is written to be inserted to the next parameter estimation procedure. For double-difference solution, a baseline is created using **SNGDIF** program, and this baseline is corrected from cycle slips for phase data using **MAUPRP** program.

The parameter estimation using the main program (**GPSEST**) is carried out through by least-square estimation (LSE) for the phase and code GNSS observations. The formulas are described in the user manual (DACH ET AL., 2007).

### **3. KINEMATIC PPP SOLUTION AND ANALYSIS STRATEGY**

Bernese software provides the possibility to obtain the PPP solutions in automatic script (Bernese Protocol Engine (BPE)). As shown in

Table 2, the used satellite orbit and clock ephemeris data from CODE center were used with intervals of 5 seconds to obtain high accurate results. Satellite and receiver phase center offsets are considered using the IGS ANTEX format (NGS, 2014), (PCV\_COD, 2014). The tropospheric correction is applied using the Global Mapping Function (GMF) model for the hydrostatic and wet delay estimation. Regarding ionospheric correction, the estimation of the PPP solution is based on the linear ionospheric free combination. Moreover, high order ionospheric parameters are used to improve the estimation.

For an accurate estimation, the ocean tidal loading correction is considered in the PPP estimation. FES (Finite Element Solution) 2004 model implemented by C. Le Provost is used by the PPP estimation (LE PROVOST & LYARD, 1997). For our data, the model parameters could be obtained through the web site of SCHERNECK (2011). The Atmosphere tidal loading is corrected by the Ray and Ponte model based on the IERS 2010 conventions (RAY & PONTE, 2003). Additionally, this correction might be obtained by GGFC (2010).

To establish the analysis strategy for this study, Figure 2 illustrates the flowchart of analysis. Some outputs of the PPP solution could be visualized, such as the satellite phase and code residuals. The high residuals might come from the lower elevation angles of the satellites. Moreover, the residuals appear due to the effect of the remaining observation errors, such as atmospheric delay, multipath or even the satellite orbit and clock residuals (CAI, 2009).

Table 2 : Bernese processing parameters

ID		Model
Reference System		ITRF2008
Coordinate format		XYZ
Satellite Orbit and clock ephemeris		CODE 5 sec interval
Satellite phase center offsets		PCV.I08 (IGS08 format)
Receiver phase center offsets		PCV.I08 (IGS08 format)
Tropospheric model	Dry model	Dry GMF
	Wet model	Wet GMF
	Mapping function	GMF
Ionospheric model		Linear ionospheric free combination
		Higher order parameters
GNSS System		GPS
Observation data		Both phase and code
Ocean tidal loading		FES2004 model
Atmosphere tidal loading		Ray and Ponte 2003 model based on ITRS 2010
Elevation angle		10°
Sampling rate		5 second

Regarding the kinematic PPP solution, the error values in the East, North and ellipsoidal height are calculated with respect to the double-difference solution from Bernese software. The Root Mean Square (RMS) error, which refers to the double-difference solution, and the standard deviation (SD), which is related to the mean value of the PPP solution error, are calculated. Furthermore, the frequency histogram is plotted.

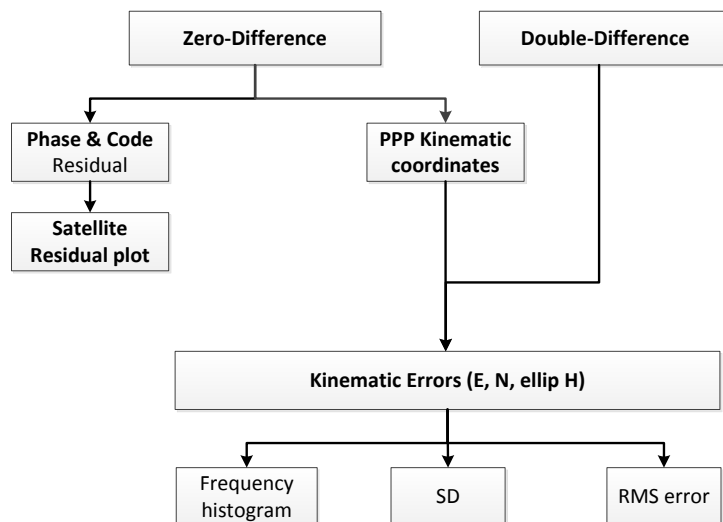


Figure 2 : Flowchart of analysis strategy

#### 4. EXPERIMENTAL WORK

Two kinematic trajectories have been observed on the Rhine River, Duisburg, Germany as a part of project “**HydrOs** - Integrated Hydrographical Positioning System”. This project is launched in co-operation between the department M5 (Geodesy) of the German Federal Institute of Hydrology (BfG) and the Institute of Engineering Geodesy at the University of Stuttgart (IIGS) (BREITENFELD ET AL., 2014).

An antenna LEIAX1203+GNSS and a receiver LEICA GX1230+GNSS are located on the surveying vessel to collect the GNSS data with an interval of 1 second during two days. Figure 3 shows the location of the GNSS antenna on the surveying vessel. The virtual SAPOS (**SA**telliten**PO**sitionierungsdienst der deutschen Landesvermessung) reference station was considered as a reference station, which was provided from SAPOS-NRW team (SAPOS-NRW, 2014). SAPOS service is collecting GNSS data around Germany (SAPOS, 2014). It is a CORS (Continuously Operating Reference Station) GNSS service; for more information about CORS, see SCHWIEGER ET AL. (2009).



Figure 3 : LEIAX1203+GNSS Antenna on the vessel  
*Photo by: Annette Scheider (IIGS)*



Table 3 shows the start and end time of the experimental works for two days [indicated by: DOY Day of Year].

Table 3 : Experimental work characteristics

Data set	Year/DOY	Start time			End time		
		hh	mm	ss	hh	mm	ss
<b>First trajectory</b>	2014/126	06	54	50	10	10	05
<b>Second trajectory</b>	2014/127	06	14	20	11	34	30

## 5. RESULTS AND DISCUSSIONS

### 5.1 First data set

The layout of the first trajectory, which was observed for more than 3 hours, is presented in Figure 4. The measurements started from the inner harbour in Duisburg. The left figure shows the overview layout and the right figure illustrates a zoom in of the trajectory below two bridges. The white line refers to the kinematic PPP trajectory; the cross white points mention to the interpolated points between two solved points from the PPP solution. Due to the loss of GNSS signals in the area of bridges, the yellow line indicates the actual vessel trajectory below bridges.

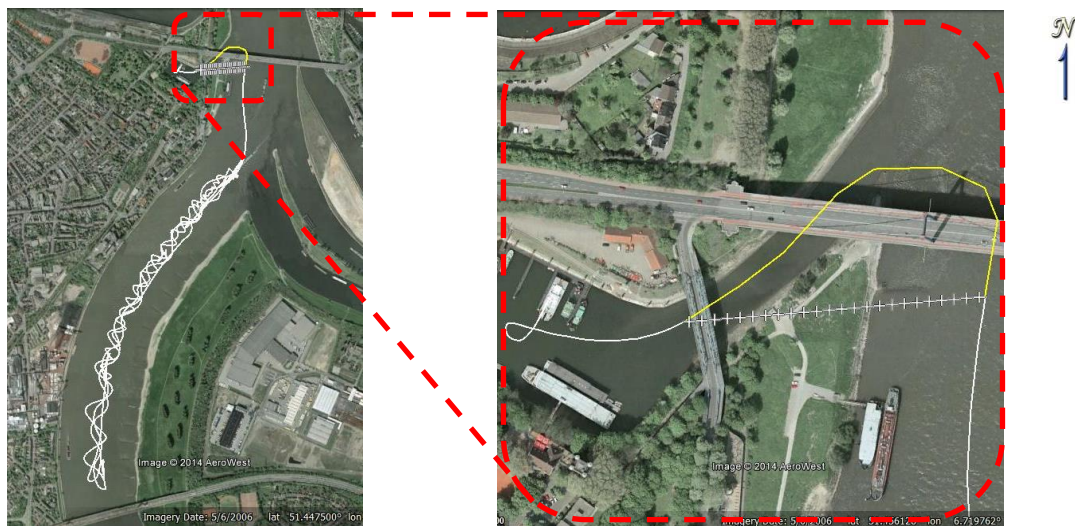


Figure 4 : Layout of the first trajectory [DOY: 2014/126] © Google Earth

As mentioned before, the double-difference solution of the Bernese software is considered as the reference solution for the PPP solution. The PPP residuals for phase and code observations (not using double-difference solution) are presented in Figure 5. In this Figure, the residual values in phase and code have a gap due to the loss of GNSS signals, which starts from epoch 438 to 486, [GPS week second = 199845: 200115]. Additionally, there are some cycle slips from epoch 883 to 892, [GPS week second = 202105: 202150].

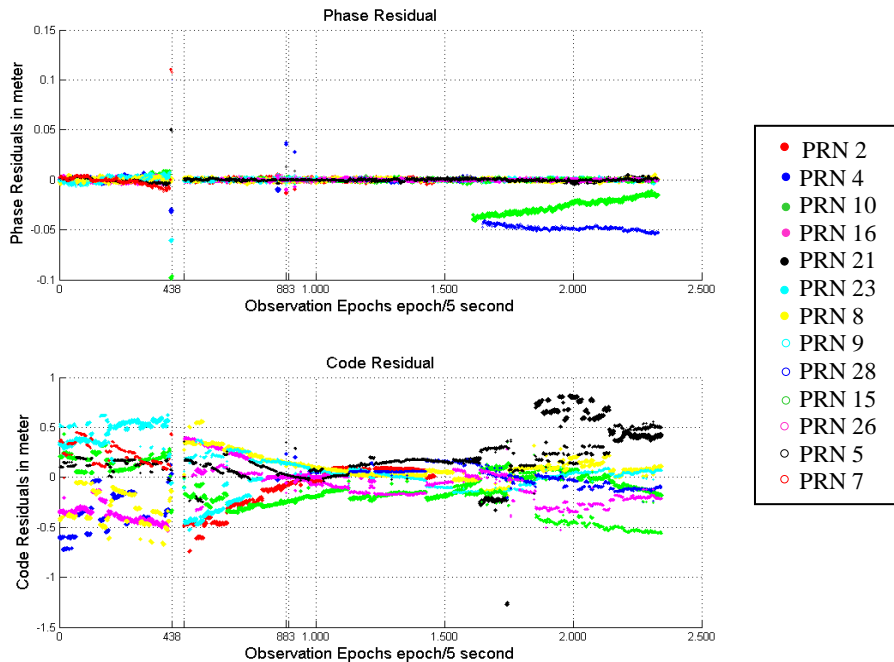


Figure 5 : Satellite residuals for the first trajectory [DOY: 2014/126]

To assess the accuracy of the PPP solution for this hydrographic trajectory, Figure 6 illustrates the analysis results for this trajectory between the double-difference and PPP solutions. The X-axis refers to the number of observations (one epoch/5 sec) and Y-axis indicates the error value in meter level. Figure (6.1) shows the error plot (m) in East, North and height. As shown previously, the error values have a gap in the solution due to the loss of lock below the bridges area. Moreover, there are some cycle slips later on, which decrease the estimated kinematic PPP accuracy.

Figure (6.2) and (6.3) provide the error plot for the East & North and East & height directions. As seen in these graphs the blue points refer to the errors and the cross red one refers to the mean value. The statistical results of PPP solution are concluded in Table 4. The kinematic PPP solution shows an RMS error of 6.40 cm in East ( $SD = 6$  cm), 4.70 cm in North ( $SD = 2.10$ ) cm and 7.10 cm in height ( $SD = 6.8$  cm).

Table 4 : Statistical results of the first trajectory [DOY: 126/2014]

	East [m]	North [m]	height [m]
Max.	0.65	0.015	0.713
Mean	0.022	-0.043	0.021
Min.	-0.163	-0.330	-1.152
RMS	0.064	0.047	0.071
SD	0.060	0.021	0.068
<b><math>SD_{95\%}</math></b>	0.050	0.012	0.050

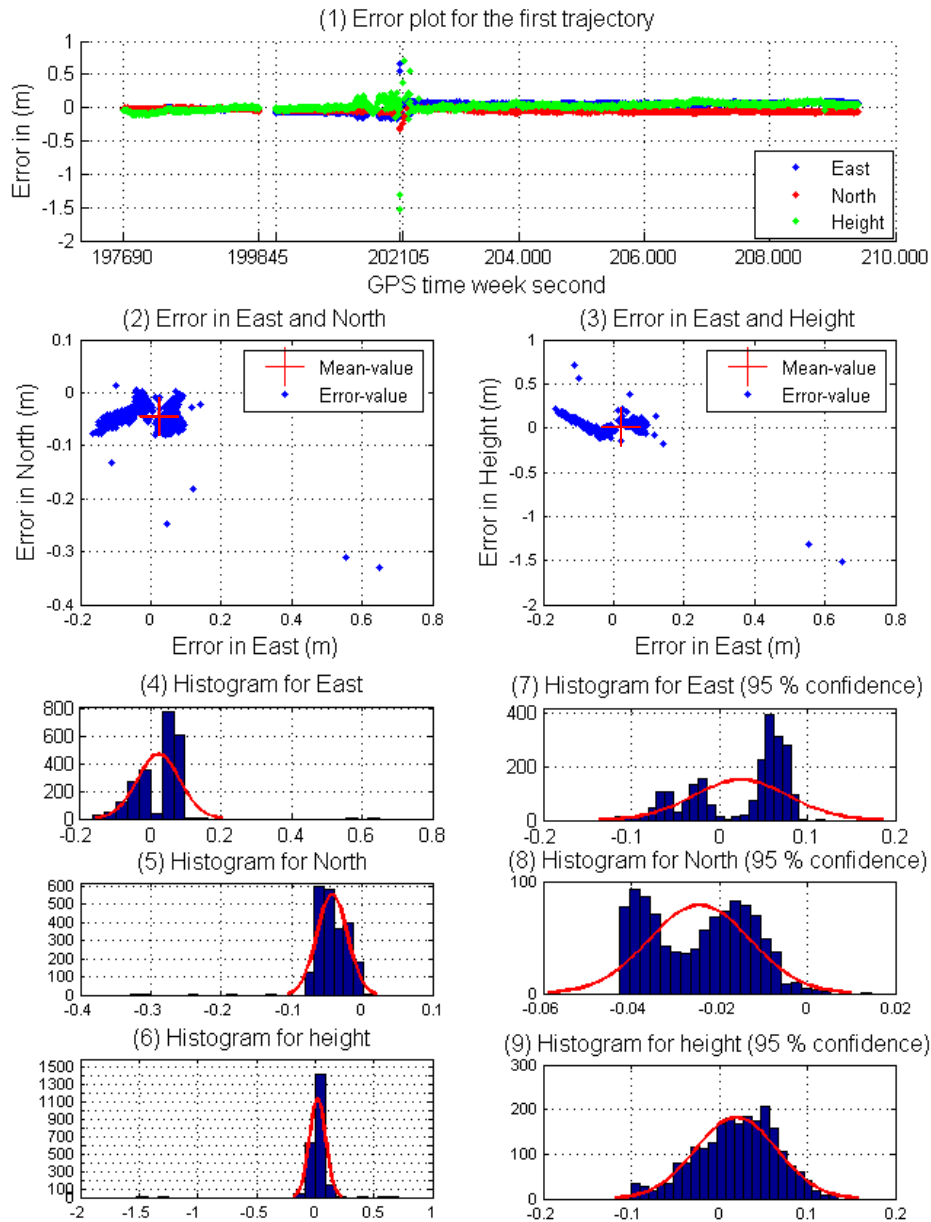


Figure 6 : Analysis results for the first trajectory [DOY: 2014/126]

A 5 % of the PPP errors are eliminated (as outliers) to get a confidence level of 95 %. The  $SD_{95\%}$  of the kinematic PPP solution is obviously improved to reach 5.0 cm, 1.20 and 5.0 cm in East, North and height directions respectively.

To distinguish between the standard deviation and the standard deviation based on the 95% confidence level, Figure 6 shows additionally the histogram of SD in Figure (6.4), (6.5), and (6.6) for East, North and height respectively. Moreover, Figure (6.7), (6.8) and (6.9) provide the error with a confidence level of 95 %. Absolutely, the error range is improved by eliminating 5 % of the data including outliers.

## 5.2 Second data set

As discussed before, the second trajectory through the Rhine River is observed in the second day [DOY: 127] for more than 5 hours, see Figure 7. 16 satellites were observed during the measurement time. In Figure 8, the phase and code residuals are plotted. Some outliers are reported in this graph which refers to cycle slips during the observations.



Figure 7 : Layout of the second trajectory, © Google Earth [DOY: 127/2014]

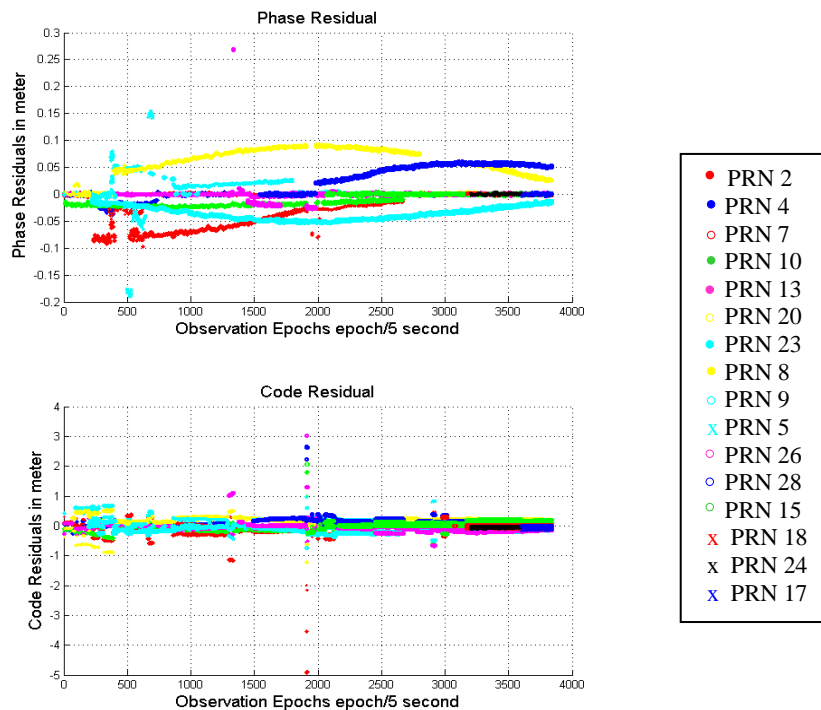


Figure 8 : Satellite residuals for the second trajectory [DOY: 127/2014]

Figure 9 illustrates the PPP results for this kinematic trajectory. Figure (9.1) shows the PPP error values in the East, North and height directions with respect to the double-difference solution from Bernese software.

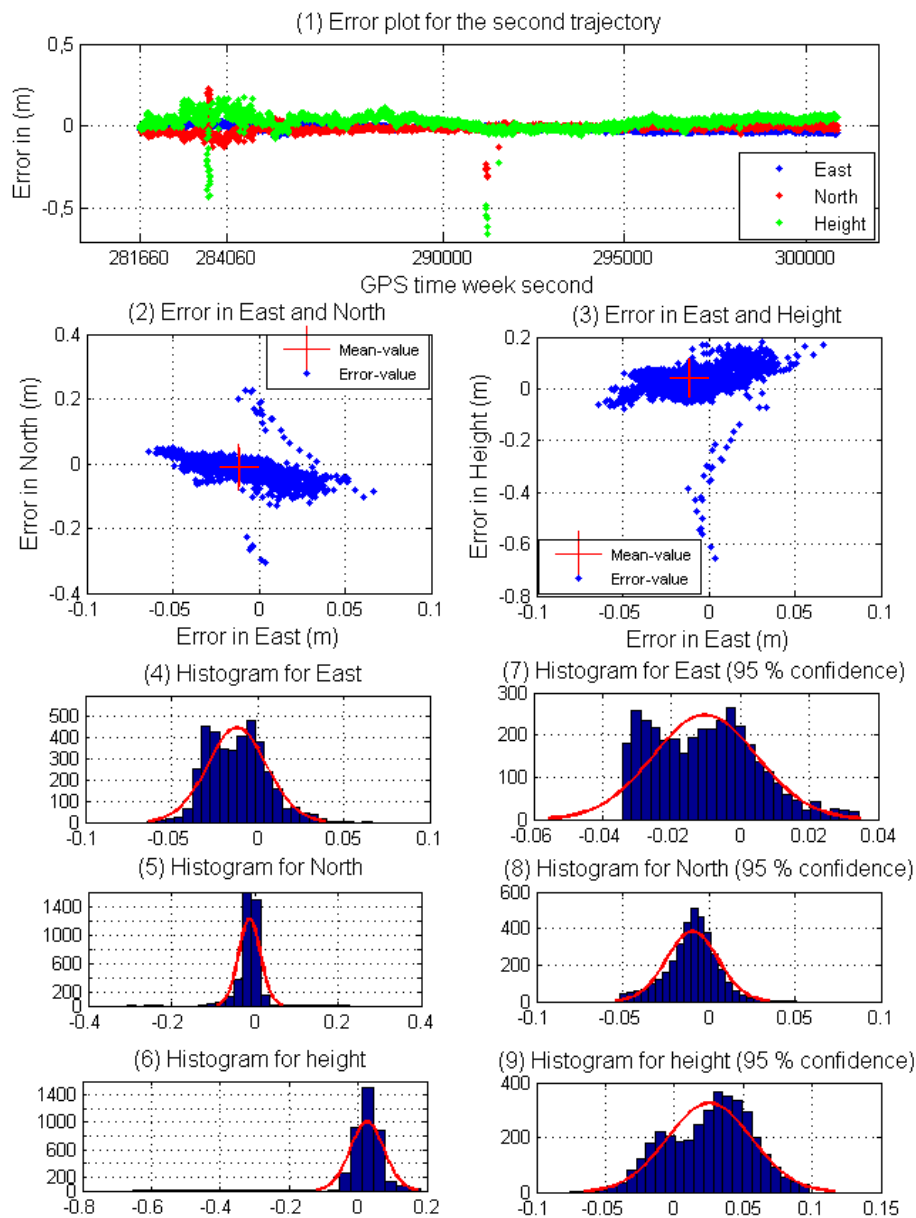


Figure 9 : Kinematic PPP solution for the second trajectory [DOY: 127/2014]

The first 40 minutes of that trajectory were realized in a quasi-static observation technique (non-moving vessel) form GPS week second 281660: 284060. The result obtained from this solution is more accurate due to the high number of satellites and the trajectory did not include the bridges area. Figure (9.2) and (9.3) show the errors in East & North and East & height.

As shown in Table 5, the maximum and minimum values for the error range, which are presented in details in Figure (9.4), (9.5) and (9.6), are reported in the East, North and height



directions. These figures show the frequency histogram for the PPP errors. From the table below, we can see that the RMS error from the solution is equal to 2.10 cm and 2.90 cm in East and North respectively. Moreover, it shows a RMS error of 5.60 cm in height. The standard deviation (SD) for these PPP errors is set out additionally in Table 5. This SD value is definitely improved after eliminating of the 5 % of the PPP errors as outliers. The standard deviation of a confidence level of 95 % ( $SD_{95\%}$ ) shows 1.5 cm in East and North and 3 cm in height. The error histograms for confidence level of the 95 % are provided in Figures (9.7), (9.8) and (9.9).

Table 5 : Statistical results of the second trajectory [DOY: 127/2014]

	East [m]	North [m]	height [m]
Max.	0.064	0.228	0.180
Mean	-0.012	-0.012	0.026
Min.	-0.064	-0.307	-0.655
RMS	0.021	0.029	0.056
SD	0.017	0.026	0.049
<b><math>SD_{95\%}</math></b>	0.015	0.015	0.030

In comparison between the two trajectories, the second trajectory provides a higher accuracy than the first trajectory. The second trajectory data has a higher number of satellites and lower outliers than the first one. It can be shown from Figure 9, that the histogram of the second trajectory is nearly similar to the Gaussian distribution curve.

## 6. CONCLUSION

The main goal of the current study was to investigate the kinematic PPP solutions for the hydrographic applications. Additionally, it aims to evaluate the suitability of using Bernese software for kinematic PPP solution in Rivers. Two kinematic trajectories have been observed on the Rhine River, Duisburg, Germany for two days. Bernese software V. 5.2 was used to obtain the kinematic PPP solution for the measurement data. The double-difference solution of Bernese software is used as reference solution for the PPP solution. The first kinematic trajectory shows a RMS error of 6.4 cm ( $SD = 6$  cm), 4.7 cm ( $SD = 2.1$  cm) and 7.1 cm ( $SD = 6.8$  cm) for East, North and height respectively. Additionally, by eliminating 5% of the PPP errors (outliers), the standard deviation ( $SD_{95\%}$ ) reports 5 cm in the East, 1.2 cm in North and 5 cm in height directions. Regarding the second trajectory, the observation starts with 40 minutes as quasi-static observation time (non-moving vessel). The accuracy achieves more accurate solution than the first trajectory. It presents a RMS error of 2.1 cm ( $SD = 1.7$  cm) in the East, 2.9 cm ( $SD = 2.6$  cm) in North and 5.6 cm ( $SD = 4.9$  cm) in height directions. This trajectory shows obvious improvement for ( $SD_{95\%}$ ) of 1.5 cm in East and North and 3 cm for height.

## ACKNOWLEDGEMENTS

The authors would like to thank Ms. Annette Scheider for receiving the GNSS measurements through the HydrOs project. Special thanks go to our partners from the BfG Mr. Harry Wirth and Mr. Marc Breitenfeld. Further thanks also for Mr. Bernhard Galitzki from SAPOS-NRW for providing us with the reference stations.

## REFERENCES

- ALKAN, R. M. & ÖCALAN, T. (2013): *Usability of the GPS Precise Point Positioning Technique in marine Applications*. Journal of Navigation, 66(4), pp. 579-588.
- BASSIRI, S. & HAJJ, G. (1993): *Higher-order ionospheric effects on the GPS observables and means of modeling them*. Manuscripta geodaetica, Springer-Verlag, 18(5), pp. 280-289.
- BÖDER, V. (2010.a): *Applications for a Hydrographic Multi Sensor System on Lakes and Rivers*. FIG Congress, 11-16 April, 2010 Sydney, Australia.
- BÖDER, V. (2010.b): *HCH-HMSS: A Multi Sensor System in Hydrographic Applications*. Bonn, Germany, Machine Control and Guidance (MCG) Conference, University of Bonn.
- BREITENFELD, M., WIRTH, H., SCHEIDER, A. & SCHWIEGER, V. (2014): *Development of a Multi-Sensor System to optimize the Positioning of Hydrographic Surveying Vessels*. MCG Conference Proceeding, Institut für Mobile Maschinen und Nutzfahrzeuge, Braunschweig, Germany, pp. 75-86.
- CAI, C. (2009): *Precise Point Positioning Using Dual-Frequency GPS and GLONASS Measurements*. M.Sc. Thesis, Calgary: University of Calgary, 2009.
- CODE (2014): *CODE ftp server*. <ftp://ftp.unibe.ch/aiub/CODE/2014/>, last accessed on October 17, 2014.
- DACH, R., FRIDEZ, P., HUGENTOBLE, U. & MEINDL, M. (2007): *User manual of the Bernese GPS Software Version 5.0*. Bern, Switzerland: Astronomical Institute, University of Bern, <http://www.bernese.unibe.ch/docs50/DOCU50.pdf>, accessed on October, 2014.
- DACH, R. & WALSER, P. (2014): *Bernese GNSS Software Version 5.2 Tutorial*. <http://www.bernese.unibe.ch/docs/TUTORIAL.pdf>, last accessed on October 17, 2014.
- GGFC (2010): *Atmosphere Tide Loading Calculator from Global Geophysical Fluid Center*. <http://geophy.uni.lu/ggfc-atmosphere/tide-loading-calculator.html>, accessed on October, 2014.
- GOA, Y. (2006): *Precise Point Positioning and its challenges*. *Inside GNSS*, Nov/Dec, 1(8), pp. 16-18.
- HESELBARTH, A. (2011): *Statische und Kinematische GNSS-Auswertung mittels Precise Point Positioning (PPP)*, Deutsche Geodätische Kommission (DKG), Reihe C, No. 667, München, Verlag der Bayerischen Akademie der Wissenschaften.
- HOFFMANN-WELLENHOF, B., LICHTENEGGER, H. & COLLINS, J. (2000): *GPS: Theory and Practics*. 4 ed. New York: Springer-Verlag/Wien.
- HOPFIELD, H. (1969): *Two-quartic topospheric refractivity profile for correcting satellite data*. Journal of Geophysical Research, 74(8), pp. 4487-4499.



- KEDER, S., HAJJ, G., WILSON, B. & HEFLIN, M. (2003): *The effect of the second order GPS ionospheric correction on receiver positions*. Geophysical Research Letters, 30(16).
- LE PROVOST, C. & LYARD, F. (1997): *Energetics of the M2 barotropic ocean tides: an estimate of bottom friction dissipation from a hydrodynamic model*. Progress in Oceanography, 40(1-4), pp. 37-52.
- LEICK, A. (1995): *GPS Satellite Surveying*. 2nd ed., Wiley, New York.
- MARINI, J. (1972): *Correction of satellite tracking data for an arbitrary tropospheric profile*. Journal of Radio Science, 7(2), pp. 223-231.
- MARREIROS, P., FERNANDES, M. J. & BASTOS, L. (2012): Evaluating the feasibility of GPS measurements of SSH on board a ship along the Portuguese West Coast. Journal of Advances in Space Research, 51(8), pp. 1492-1501.
- MELBOURNE, W. G. (1985): *The Case for Ranging in GPS Based Geodetic Systems*. In: Proceedings : First International Symposium on Precise Positioning with the Global Positioning System. US Department of Commerce, Rockville, Maryland: Penn State University, pp. 373-386.
- MIRSA, P. & ENGE, P. (2010): *Global Positioning System Signals, Measurements, and Performance*. Revised second ed., Ganga-Jamuna Press.
- MOREIRA, D. et al. (2012): Applications of GNSS data for hydrological studies in the Amazon basin. European Geosciences Union, 22-27 April, 2012, Vienna, Austria.
- NGS, (2014): *Antenna Absolute Calibrations*. <http://www.ngs.noaa.gov/ANTCAL/>, last accessed on October 15, 2014.
- NIELL, A. (1992): Global mapping functions for the atmosphere delay at radio wavelengths. *Journal of Geophysical Research*, 101(B1), pp. 3227-3246.
- PCV\_COD (2014): *Phase Center Variation from CODE ftp server*. [ftp://ftp.unibe.ch/aiub/BSWUSER52/GEN/PCV\\_COD.I08](ftp://ftp.unibe.ch/aiub/BSWUSER52/GEN/PCV_COD.I08), last accessed on October 15, 2014.
- RAY, R. D. & PONTE, R. M. (2003): *Barometric tides from ECMWF operational analyses*. Annales Geophysicae, 21, pp. 1897-1910.
- SAASTAMOINEN, J. (1973): *Contribution to the theory of atmospheric refraction*. Bulletin géodésique, 107(1), pp. 13-34.
- SAPOS, 2014. *SAPOS*. <http://www.sapos.de/>, last accessed on October 15, 2014.
- SAPOS-NRW, 2014. *SAPOS-NRW*. <http://www.sapos.nrw.de/>, last accessed on October 15, 2014.
- SCHERNECK, H.G. (2011): *Chalmers/Onsala Space Observatory*. <http://holt.oso.chalmers.se/loading/>, last accessed on October 10, 2014.
- SCHWIEGER, V., LILJE, M. & SARIB, M. (2009): *GNSS CORS – Reference Frames and Services*. 7th FIG Regional Conference, Hanoi, Vietnam,
- WÜBBENA, G. (1985): *Software Developments for Geodetic Positioning with GPS Using TI 4100*. In: Proceedings First International Symposium on Precise Positioning with the Global Positioning System. US Department of Commerce, Rockville, Maryland: Penn State University, pp. 403–412.

## BIOGRAPHICAL NOTES

### M. Sc. Ashraf Abdallah

- 1998 – 2003 Studies of Civil Engineering in Aswan (University of Aswan, Egypt)
- 2005 – 2009 Research associate in Civil Engineering in Aswan (University of Aswan, Egypt)
- 2009 Master of Science (University of Aswan, Egypt)
- 2009 – 2011 Assistant lecturer in Civil Engineering in Aswan (University of Aswan, Egypt)
- 2012 Ph. D. student at Institute of Engineering Geodesy, University of Stuttgart

### Prof. Dr.-Ing. habil. Volker Schwieger

- 1983 – 1989 Studies of Geodesy in Hannover
- 1989 Dipl.-Ing. Geodesy (University of Hannover)
- 1998 Dr.-Ing. Geodesy (University of Hannover)
- 2004 Habilitation (University of Stuttgart)
- 2010 Professor and Head of Institute of Engineering Geodesy, University of Stuttgart
- 2015 Chair of FIG Commission 5 ‘Positioning and Measurement’

## CONTACTS

### M. Sc. Ashraf Abdallah

Institute of Engineering Geodesy, University of Stuttgart  
Geschwister-Scholl-Str. 24D  
70174 Stuttgart  
GERMANY  
Tel. + 49 711 68584051  
Fax + 49 711 68584044  
Email: [ashraf.abdallah@ingeo.uni-stuttgart.de](mailto:ashraf.abdallah@ingeo.uni-stuttgart.de)  
Web site: [www.uni-stuttgart.de/ingeo](http://www.uni-stuttgart.de/ingeo)